Cell Reports

Renal Fanconi Syndrome Is Caused by a Mistargeting-Based Mitochondriopathy

Graphical Abstract

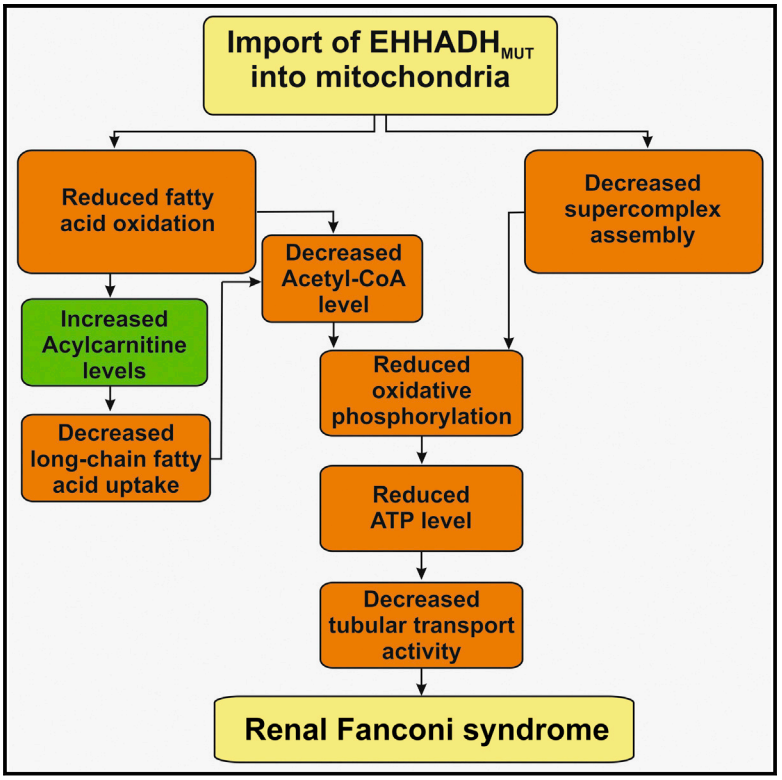

Highlights

- Mitochondriopathy due to mistargeted peroxisomal protein
- Impaired mitochondrial fatty acid β-oxidation and oxidative phosphorylation
- Decreased respiratory supercomplex formation

Authors

Nadine Assmann, Katja Dettmer, Johann M.B. Simbuerger, ..., Peter J. Oefner, Markus Reichold, Joerg Reinders

Correspondence

joerg.reinders@ukr.de

In Brief

Assmann et al. examine the molecular mechanism underlying a recently described Fanconi syndrome. Mistargeting of the peroxisomal protein EHHADH to mitochondria leads to impaired mitochondrial fatty acid β-oxidation and respiration, resulting in decreased ATP production. Diminished transport activity leads to the observed Fanconi syndrome.

Assmann et al., 2016, Cell Reports *15*, 1423–1429
May 17, 2016
http://dx.doi.org/10.1016/j.celrep.2016.04.037

CellPress

Cell Reports
Report

Renal Fanconi Syndrome Is Caused by a Mistargeting-Based Mitochondriopathy

Nadine Assmann,[1] Katja Dettmer,[1] Johann M.B. Simbuerger,[1] Carsten Broeker,[2] Nadine Nuernberger,[1] Kathrin Renner,[4] Holly Courtneidge,[3] Enriko D. Klootwijk,[3] Axel Duerkop,[6] Andrew Hall,[5] Robert Kleta,[3] Peter J. Oefner,[1] Markus Reichold,[2,7] and Joerg Reinders[1,7,*]

[1]Institute of Functional Genomics, University of Regensburg, 93053 Regensburg, Germany
[2]Medical Cell Biology, University of Regensburg, 93053 Regensburg, Germany
[3]Centre for Nephrology, University College London, London NW3 2PF, UK
[4]Department of Hematology and Oncology, University Clinic Regensburg, 93053 Regensburg, Germany
[5]Institute of Anatomy, University of Zurich, 8057 Zurich, Switzerland
[6]Institute of Analytical Chemistry, University of Regensburg, 93053 Regensburg, Germany
[7]Co-senior author
*Correspondence: joerg.reinders@ukr.de
http://dx.doi.org/10.1016/j.celrep.2016.04.037

SUMMARY

We recently reported an autosomal dominant form of renal Fanconi syndrome caused by a missense mutation in the third codon of the peroxisomal protein EHHADH. The mutation mistargets EHHADH to mitochondria, thereby impairing mitochondrial energy production and, consequently, reabsorption of electrolytes and low-molecular-weight nutrients in the proximal tubule. Here, we further elucidate the molecular mechanism underlying this pathology. We find that mutated EHHADH is incorporated into mitochondrial trifunctional protein (MTP), thereby disturbing β-oxidation of long-chain fatty acids. The resulting MTP deficiency leads to a characteristic accumulation of hydroxyacyl- and acylcarnitines. Mutated EHHADH also limits respiratory complex I and corresponding supercomplex formation, leading to decreases in oxidative phosphorylation capacity, mitochondrial membrane potential maintenance, and ATP generation. Activity of the Na^+/K^+-ATPase is thereby diminished, ultimately decreasing the transport activity of the proximal tubule cells.

INTRODUCTION

Fanconi syndrome is a disorder of the proximal kidney tubule. It is characterized by failure of the proximal tubule to reabsorb filtered molecules, causing urinary loss of amino acids, glucose, electrolytes, phosphate, and low-molecular-weight proteins. Klootwijk et al. (2014) recently described a new form of inherited Fanconi syndrome caused by mutation of the *EHHADH* gene, which is highly expressed in human liver and kidney (Hoefler et al., 1994). EHHADH (enoyl-coenzyme A hydratase/L-3-hydroxyacyl-coenzyme A dehydrogenase) is a peroxisomal protein involved in β-oxidation of fatty acids. Mutation at p.E3K results in a de novo mitochondrial import sequence, resulting in mistargeting to mitochondria. The mutated protein interferes with mitochondrial energy production, which is predominantly based on fatty acid oxidation (FAO) in proximal tubular cells, leading to Fanconi syndrome.

Peroxisomes are the site of initial β-oxidation for very-long-chain and branched-chain fatty acids. In contrast, long-chain fatty acids, constituting the main source of energy under physiological conditions (Reddy and Hashimoto, 2001), are oxidized in the mitochondria by the mitochondrial trifunctional protein (MTP). The MTP is a hetero-octamer composed of four α and four β subunits and is bound to the inner mitochondrial membrane. The α subunit (HADHA) catalyzes the first steps of β-oxidation (hydration and dehydrogenation), whereas the β subunit (HADHB) facilitates the thiolytic cleavage step.

Mitochondrial FAO disruption leads to export of acylcarnitines to the extracellular fluid (Ventura et al., 1998; Violante et al., 2013). Consequently, plasma acylcarnitine levels are currently a key biomarker for neonatal screening of mitochondrial FAO disorders (Rinaldo et al., 2008).

Reducing equivalents, which are formed during the β-oxidation cycle, are fed into mitochondrial oxidative phosphorylation, and it has been shown that accumulation of β-oxidation intermediates impairs and possibly uncouples mitochondrial oxidative phosphorylation (Ho and Pande, 1974; Shrago et al., 1995; Ventura et al., 1995, 1996; Tonin et al., 2013). Mitochondrial supercomplexes, wherein the respiratory chain complexes I, III, and IV associate with each other in varying ratios, are also known to interact with FAO complexes (Wang et al., 2010). These supercomplexes mediate direct electron transfer and thus more efficient oxidative phosphorylation. Mitochondrial fatty acid β-oxidation and oxidative phosphorylation are therefore tightly coupled processes.

The transport activity of the proximal tubule is highly dependent on ATP to supply sufficient energy for Na^+/K^+-ATPase to build up the electrochemical gradient (Balaban et al., 1980), which drives resorption of solutes from the primary urine in the proximal tubule (Curthoys and Moe, 2014). This paper,

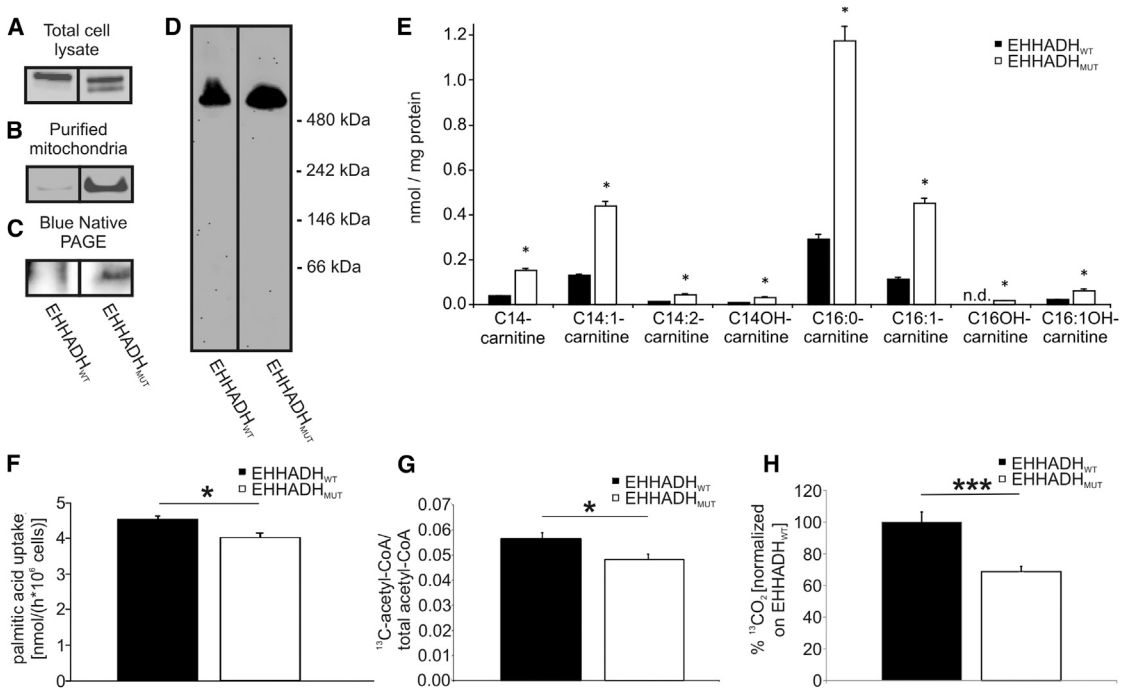

Figure 1. Mislocalization of EHHADH$_{MUT}$ and Effect on FAO

(A) Immunoblot analysis of total cell lysate against EHHADH shows an additional band ~2.5 kDa lower in molecular mass in *EHHADH$_{MUT}$* cells, indicating an N-terminal truncation upon import into mitochondria.

(B) Immunoblot analysis of purified mitochondria against EHHADH. Mitochondrial localization of the truncated but not the full-length EHHADH$_{MUT}$ is shown by immunoblot analysis of purified mitochondria, whereas EHHADH$_{WT}$ is not imported into mitochondria.

(C) In the BN-PAGE-immunoblot against EHHADH, a band is observed at ~500 kDa in *EHHADH$_{MUT}$* cells, corresponding to the expected mass of the native MTP complex, indicating the interaction of EHHADH$_{MUT}$ with the MTP complex. In contrast, no band is observed for *EHHADH$_{WT}$* cells.

(D) BN-PAGE-immunoblot analysis against HADHB shows a band at the expected ~500 kDa in both *EHHADH$_{MUT}$* and *EHHADH$_{WT}$* cells, pointing toward an exchange of EHHADH$_{MUT}$ for the α subunit.

(E) Increased amounts of long-chain acylcarnitines were found in *EHHADH$_{MUT}$* cells compared with *EHHADH$_{WT}$* cells, indicating abnormal β-oxidation of long-chain fatty acids (n = 4). n.d., not detected.

(F) Decreased palmitic acid uptake rate in *EHHADH$_{MUT}$* cells (n = 4).

(G) Decreased amount of 1,2-^{13}C-labeled acetyl-coenzyme A derived from FAO in *EHHADH$_{MUT}$* compared with *EHHADH$_{WT}$* cells (n = 3).

(H) Diminished amount of $^{13}CO_2$ produced by the *EHHADH$_{MUT}$* cell line (n = 3).

Values are mean ± SEM. *p ≤ 0.05, ***p ≤ 0.001.

employing a combination of cell biological, biochemical, proteomic, and metabolomic methods, aims to elucidate how mitochondrial mislocalization of EHHADH leads to Fanconi syndrome.

RESULTS

Subcellular Localization of Mutated EHHADH

The p.E3K-mutation of EHHADH$_{MUT}$ leads to the generation of an N-terminal mitochondrial targeting sequence in addition to the native C-terminal peroxisomal targeting sequence (Klootwijk et al., 2014). Therefore, EHHADH$_{MUT}$ localizes to both peroxisomes and mitochondria. Upon import into mitochondria, the mitochondrial targeting sequence is cleaved, resulting in an N-terminally truncated form of EHHADH, as evidenced by anti-EHHADH immunoblot analysis (Figure 1A), which shows an additional band for the *EHHADH$_{MUT}$* cells. Consequently, only the truncated form is observed in an immunoblot of isolated mitochondria from *EHHADH$_{MUT}$* cells, whereas only a faint band is observed for mitochondria of the *EHHADH* wild-type (*EHHADH$_{WT}$*) cells (Figure 1B), presumably caused by minor mislocalization of overexpressed EHHADH$_{WT}$. Respective loading controls using marker proteins are shown in Figure S1.

Interaction Analysis of Mislocalized EHHADH$_{MUT}$ in Mitochondria

Co-immunoprecipitation against EHHADH from purified mitochondria and subsequent GeLC-MS/MS identified HADHA and HADHB, both subunits of the MTP complex, as potential interaction partners, confirming our previous co-immunoprecipitation results using an HADHB antibody (Klootwijk et al., 2014). To investigate this interaction in more detail, a blue native (BN) PAGE of mitochondrial protein complexes isolated from *EHHADH$_{MUT}$* and *EHHADH$_{WT}$* cells with subsequent immunoblotting against EHHADH and HADHB was performed. In *EHHADH$_{MUT}$* cells, a band was observed at ~500 kDa, corresponding to the native MTP complex, indicating the interaction

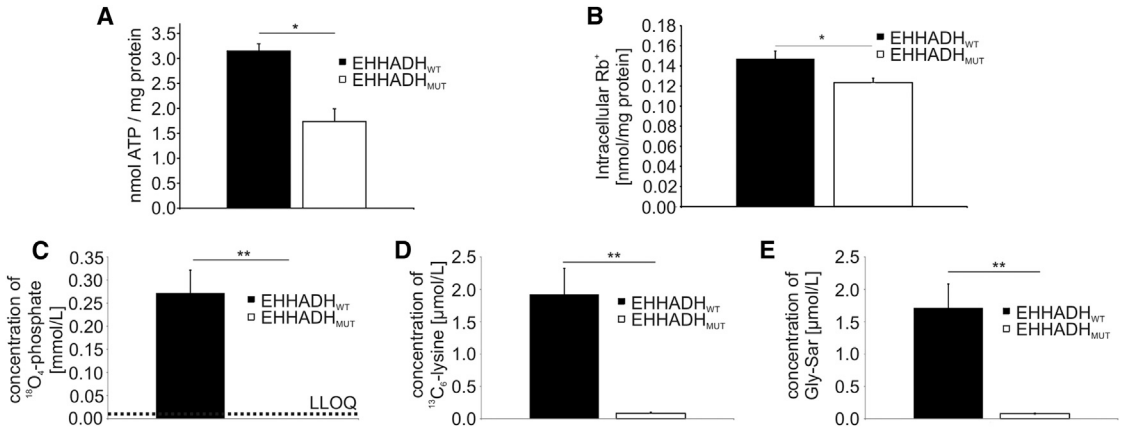

Figure 2. Cellular Energy Supply and Transport Activity

(A) The cellular ATP level is significantly reduced in *EHHADH*$_{MUT}$ cells (n = 4).

(B) The activity of Na^+/K^+-ATPase generating the driving force for transcellular transport is significantly diminished (n = 5).

(C–E) The transcellular transport of all tested solutes within 8 hr (C, ^{18}O-phosphate; D, $^{13}C_6$-lysine; E, Gly-Sar-dipeptide) is reduced by more than 90% in *EHHADH*$_{MUT}$ cells. The values for ^{18}O-phosphate were below the lower limit of quantification (LLOQ, indicated by the dotted line) for *EHHADH*$_{MUT}$ cells (n = 6). Values are mean ± SEM. *p ≤ 0.05, **p ≤ 0.01.

of EHHADH$_{MUT}$ with the MTP complex. In contrast, no band was observed for *EHHADH*$_{WT}$ cells (Figure 1C). Moreover, the band for HADHB was found at the expected ~500 kDa in both *EHHADH*$_{WT}$ and *EHHADH*$_{MUT}$ cells (Figure 1D). No mass shift was observed in the BN PAGE immunoblot against HADHB, suggesting replacement of one or more α subunits (~79 kDa) of the MTP complex with EHHADH$_{MUT}$ (~77 kDa), which are of similar molecular mass, rather than replacement of much smaller β subunits (~51 kDa) or additional attachment of EHHADH$_{MUT}$ to the MTP complex.

Metabolic Analysis

Accumulation of acylcarnitines and hydroxyacylcarnitines because of impaired β-oxidation is a diagnostic marker of MTP deficiencies. The amounts of tetradecanoyl- and hexadecanoylcarnitine as well as their corresponding ketoacyl- and hydroxyacylcarnitines were significantly elevated in *EHHADH*$_{MUT}$ cells. The concentration of hydroxyhexadecanoylcarnitine in *EHHADH*$_{WT}$ cells was even below the detection limit (Figure 1E). The reduced FAO, in turn, leads to significantly reduced uptake of fatty acids from the medium (Figure 1F; p = 0.016; Eaton, 2002; Hirschey et al., 2010). Also, the level of FAO-derived acetyl-coenzyme A (CoA) was lower in *EHHADH*$_{MUT}$ than in *EHHADH*$_{WT}$ cells (Figure 1G; p = 0.044) using U-^{13}C-labeled palmitic acid as the primary energy source. This finding is further corroborated by a significant decrease in $^{13}CO_2$-production by *EHHADH*$_{MUT}$ cells (Figure 1H; $p = 4.4 \times 10^{-5}$). Consequently, a significant 45% reduction in ATP content was found in *EHHADH*$_{MUT}$ cells (Figure 2A; p = 0.012), indicating a reduced energy supply. Markedly, the decrease in ATP level in the *EHHADH*$_{MUT}$ cells did not result in a significant increase in apoptosis within the 7-day stimulation period (data not shown). However, extending the expression of mutated EHHADH for 3 more days resulted in a significant increase in the fraction of apoptotic *EHHADH*$_{MUT}$ cells compared with *EHHADH*$_{WT}$ cells (Figure S2; $p = 4.6 \times 10^{-8}$).

Activity of Na^+/K^+-ATPase and Diminished Transcellular Transport

Uptake of Rb^+, as a surrogate substrate for Na^+/K^+-ATPase, was measured by inductively coupled plasma-optical emission spetroscopy (ICP-OES). The activity of Na^+/K^+-ATPase was significantly reduced in the *EHHADH*$_{MUT}$ cell line (Figure 2B; p = 0.023). As a consequence, the transcellular transport of phosphate (p = 0.005), lysine (p = 0.002), and the dipeptide Gly-Sar (p = 0.002) in *EHHADH*$_{MUT}$ cells was reduced more than 20-fold compared with *EHHADH*$_{WT}$ cells (Figures 2C and 2D).

High-Resolution Respirometry and Confocal Microscopy

High-resolution respirometry revealed a significantly reduced oxidative phosphorylation capacity of *EHHADH*$_{MUT}$ cells after addition of palmitoylcarnitine and malate (electron transfer flavoprotein $[ETF]_{OXPHOS}$) as substrates for β-oxidation. The respective results are shown in Figure 3A, top. Addition of substrates for complex I (CI_{OXPHOS}) resulted in no further increase in oxygen consumption, with *EHHADH*$_{MUT}$ cells still showing decreased oxygen consumption. After addition of substrate for complex II ($CI+II+ETF_{OXPHOS}$) and at maximum oxidative phosphorylation in a coupled state, *EHHADH*$_{MUT}$ cells showed significantly reduced oxidative phosphorylation, and the oxygen consumption linked to ATP (O_2-ATP CI+II+ETF) was reduced by 22%. After uncoupling, respiration rose similarly, ~0.06 pmol/(s*ml*citrate synthase unit) in both *EHHADH*$_{WT}$ and *EHHADH*$_{MUT}$ cells, and the latter still showed decreased respiration, indicating that not only the oxidative phosphorylation machinery but also the electron transport system were impaired. After inhibition of complex I (CII ETS), the uncoupled complex II respiration was still significantly reduced in *EHHADH*$_{MUT}$ cells. Remarkably, use of octanoyl- instead of palmitoylcarnitine did not result in a substantial change of the results (Figure 3A, bottom). In concordance with the reduced respiratory activity of the *EHHADH*$_{MUT}$ cells, the mitochondrial membrane potential was reduced

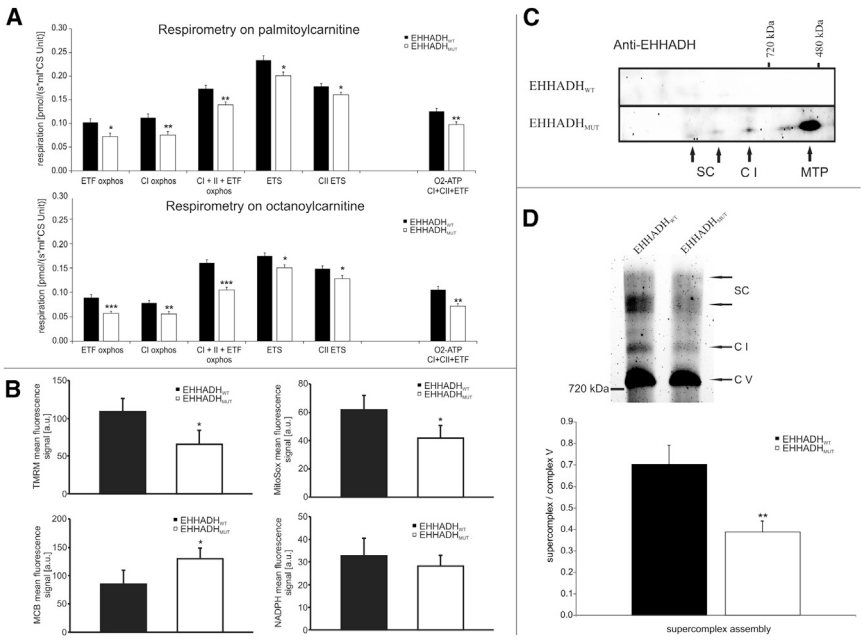

Figure 3. Results of High-Resolution Respirometry Analysis, Confocal Microscopy, and BN PAGE

(A) Significantly reduced respiration in *EHHADH*$_{MUT}$ cells after the addition of substrates for ETF (top, palmitoylcarnitine; bottom, octanoylcarnitine), complex I, and complex II compared with *EHHADH*$_{WT}$ cells. After inhibition of ATP synthase (LEAK) and uncoupling (ETS and CII ETS), *EHHADH*$_{MUT}$ cells show significantly reduced levels of respiration, indicating a dysfunction in both the phosphorylation and non-phosphorylation part of the respiratory chain. Use of octanoylcarnitine instead of the typical MTP substrate palmitoylcarnitine did not result in enhanced mitochondrial respiration. Values are mean ± SEM, normalized to citrate synthase (CS) activity (n = 10).

(B) The mitochondrial membrane potential ($\Delta\psi_m$), measured by tetramethylrhodamine, was significantly greater in *EHHADH*$_{WT}$ than in *EHHADH*$_{MUT}$ cells (top left). ROS production, measured with the mitochondrially targeted superoxide probe MitoSOX, was significantly higher in *EHHADH*$_{WT}$ cells (top right), whereas glutathione levels, measured using monochlorobimane, were significantly higher in *EHHADH*$_{MUT}$ cells (bottom left). No significant difference was found in mitochondrial NAD(P)H signal (bottom right).

(C) Immunoblot analysis against EHHADH in mitochondrial complexes separated by 2D BN/SDS-PAGE. Incorporation of mutated EHHADH into the respiratory chain complex I (CI), supercomplexes (SC), and solitary MTPs) is demonstrated.

(D) Exemplary BN PAGE of mitochondria isolated from *EHHADH*$_{WT}$ and *EHHADH*$_{MUT}$ cells, respectively, stained with lava purple for quantification (top). Densitometric analysis of supercomplex assembly in *EHHADH*$_{WT}$ and *EHHADH*$_{MUT}$ cells (bottom) reveals a reduced level of supercomplex assembly in the latter. Values are mean ± SEM, normalized to complex V (n = 7).

*p ≤ 0.05, **p ≤ 0.01, ***p ≤ 0.001.

(Figure 3B, top left). Consequently, the generation of mitochondrial reactive oxygen species (ROS) was reduced (Figure 3B, top right), and glutathione levels were higher in the *EHHADH*$_{MUT}$ cells (Figure 3B, bottom left). Therefore, no signs of increased oxidative stress were obtained in the mutant, and no change in the mitochondrial nicotinamide adenine dinucleotide(phosphate) (NAD(P)H) signal was observed in confocal microscopy (Figure 3B, bottom right).

Differential Proteomic Analysis of Whole-Cell Lysates

The differential proteomic analysis by sequential window acquisition of all theoretical fragment-ion spectra (SWATH)-MS revealed significant downregulation of several constituents of complex I of the respiratory chain (six of the nine identified subunits are significantly downregulated; Table S3). All other respiratory chain complexes showed either no regulation or no clear trend in regulation. Furthermore, several proteins involved in fatty acid β-oxidation were significantly regulated, including peroxisomal bifunctional enzyme isoform 1 (EHHADH) and acyl-CoA binding protein, which were significantly upregulated in *EHHADH*$_{MUT}$ cells.

Respiratory Supercomplex Assembly

2D BN/SDS-PAGE immunoblot analysis against EHHADH in *EHHADH*$_{MUT}$ cells showed an association of mutated EHHADH with respiratory complexes, whereas no association was visible in *EHHADH*$_{WT}$ cells (Figure 3C). Furthermore, incorporation of mutated EHHADH into the solitary MTP complex, indicated by a band at the expected height of ~500 kDa, is once again observed (see also Figure 1D). Densitometric analysis of the BN PAGE showed that *EHHADH*$_{MUT}$ cells contained markedly less supercomplex than *EHHADH*$_{WT}$ cells (Figure 3D; p = 0.009).

DISCUSSION

This paper aimed to elucidate the molecular consequences of the mistargeting of the peroxisomal protein EHHADH into mitochondria, causing an isolated autosomal dominant Fanconi's syndrome.

Mislocalization to the mitochondria and truncation of EHHADH$_{MUT}$ by the mitochondrial import machinery was shown by means of immunoblot analysis of isolated mitochondria. Moreover, the mutated untruncated form is still localized to its genuine compartment, the peroxisome; thus, peroxisomal FAO presumably remains unaffected. This is in concordance with our previous report showing that the p.E3K mutation results in a de novo mitochondrial import sequence that mistargets EHHADH$_{MUT}$ into mitochondria, and no indications of disturbance of the peroxisomal FAO in the patients were obtained (Klootwijk et al., 2014). Furthermore, EHHADH$_{MUT}$ was found to associate with MTP. The absence of a mobility shift in BN PAGE between native MTP and EHHADH$_{MUT}$ containing MTP suggests the incorporation of EHHADH$_{MUT}$ into MTP, likely in exchange for an original α subunit, instead of mere attachment to the hetero-octameric complex or exchange of a much smaller β subunit.

Incorporation of mislocalized $EHHADH_{MUT}$ into MTP leads to impaired β-oxidation of long-chain fatty acids, causing, in turn, increased levels of long-chain acylcarnitines, which is a well-known clinical parameter for FAO disorders (Rinaldo et al., 2008). The acylcarnitine profile of *EHHADH*$_{MUT}$ cells showed an increase in long-chain 2-enoyl-, hydroxy-acyl-, and acylcarnitines, resembling the situation in patients with long chain 3-hydroxyacyl-CoA dehydrogenase (LCHAD) or MTP deficiency (Sander et al., 2005). This lends further support to an impaired β-oxidation of long-chain fatty acids by incorporation of $EHHADH_{MUT}$ into the MTP.

The major source for energy generation in proximal tubular cells is oxidative metabolism, mostly from fatty acids (Epstein, 1997). Beck et al. (1991) showed a decrease in the intracellular ATP level after stimulation of sodium transport in isolated rabbit proximal convolute tubules, indicating that physiological ATP levels in proximal tubular cells barely suffice to meet cellular energy demands. Although the levels of intracellular ATP in *EHHADH*$_{WT}$ cells agree with published data (Andreoli and Mallett, 1997; Balaban et al., 1980; Migita et al., 2007), *EHHADH*$_{MUT}$ cells showed a marked decrease in intracellular ATP level. This decrease also fits the concept of disturbed β-oxidation because of the mistargeting of $EHHADH_{MUT}$ into mitochondria.

Disturbance of β-oxidation will also affect the uptake of fatty acids and production of acetyl-CoA as the end product of β-oxidation. We observed a decreased uptake in *EHHADH*$_{MUT}$ cells. Furthermore, an increase in long-chain acylcarnitines leads to export from mitochondria instead of an import of long-chain acyl-CoAs. In SWATH-MS analysis, an increased amount of acyl-CoA binding protein was found. This could be due to an increase in long-chain acyl-CoAs in the cytosol of *EHHADH*$_{MUT}$ cells counteracting the higher cytosolic long-chain acyl-CoA concentration. More probable is that lack of ATP impairs the activation of imported fatty acids to form long-chain acyl-CoAs (Eaton, 2002) and, thereby, lowers the uptake of long-chain fatty acids. Taken together, the accumulation of intermediates of β-oxidation leads to product inhibition and, thereby, decreases both mitochondrial β-oxidation flux and the amount of acetyl-CoA, CO_2, and, consequently, ATP produced by degradation of fatty acids.

The mitochondrial respiratory chain and mitochondrial β-oxidation are tightly coupled processes. A physical association between mitochondrial fatty acid β-oxidation and respiratory chain complexes via MTP was shown by Wang et al. (2010). The mistargeting of $EHHADH_{MUT}$ into mitochondria leads to its incorporation into MTP and subsequent incorporation into the respiratory supercomplexes, as shown by immunoblot analysis of 2D BN/SDS-PAGE (Figure 3C). Supercomplex assembly in *EHHADH*$_{MUT}$ cells was decreased compared with that in *EHHADH*$_{WT}$ cells. Therefore, the erroneous incorporation of mutated EHHADH into MTP might lead to a conformational change in the fatty acid β-oxidation complex and, thus, to an impaired supercomplex assembly, resulting in degradation of individual subunits, as indicated by the decrease in abundance of several subunits of complex I of the respiratory chain. The formation of supercomplexes in the mitochondrial inner membrane features some functional advantages because it mediates substrate channeling, increases electron transfer rates, shows higher catalytic efficiency, sequesters reactive intermediates, and, in addition, stabilizes respiratory chain complexes (Schägger, 2001). Thus, a decrease in mitochondrial respirasome assembly will lead to a decrease in oxidative phosphorylation capacity, as shown by Rosca et al. (2008). We also observed a decreased oxidative phosphorylation capacity in *EHHADH*$_{MUT}$ cells. The dysfunction in the oxidative phosphorylation system is located in both the phosphorylation and non-phosphorylation system because the *EHHADH*$_{MUT}$ cells still showed decreased oxygen consumption after inhibition of ATP synthase and uncoupling. In patients with mere MTP deficiency, substitution of dietary long-chain fat with medium-chain triglycerides will alleviate clinical symptoms (Saudubray et al., 1999; Gillingham et al., 2006) because medium-chain triglycerides can enter mitochondria independently of carnitine and bypass the long-chain β-oxidation enzymes. In contrast, the substitution of palmitoylcarnitine with octanoylcarnitine in respirometric analysis of *EHHADH*$_{MUT}$ cells did not normalize but merely led to a less pronounced decrease in respiratory activity (Figure 3A). Therefore, the direct effects on assembly and activity of the respiratory chain make a substantial contribution to the decrease in ATP production in addition to the diminished FAO, which may, at least in part, be compensated by other energy-producing processes.

The production of ATP is essential for maintaining the activity of Na^+/K^+-ATPase, which is responsible for generation of the electrochemical gradient across the plasma membrane, required for renal tubular reabsorption. Therefore, the decreased ATP level in *EHHADH*$_{MUT}$ cells leads to lower activity of Na^+/K^+-ATPase, as shown by uptake of Rb^+ as a K^+ surrogate. Consequently, transport of all tested solutes across proximal tubular cells was drastically decreased, inducing Fanconi syndrome and the clinical symptom of rickets caused by the loss of phosphate. These findings are in accordance with the previously published decrease in glucose transport activity (Klootwijk et al., 2014). The fact that no other clinically relevant symptoms are caused by EHHADH mislocalization is presumably due to the particularly high expression of EHHADH in the late proximal tubule and the high energy demand of the proximal tubule cells, which is for the most part covered by FAO (Epstein, 1997).

Subsequent studies will be focused on physiological analyses in vivo as conducted for other proximal tubular disorders; e.g., using a respective knockin mouse model (Novarino et al., 2010) or primary cell culture (Gorvin et al., 2013; Ivanova et al., 2015) if patient material is available.

Conclusions

Mistargeting of $EHHADH_{MUT}$ to mitochondria impairs mitochondrial fatty acid β-oxidation and respiration because of interaction and interference with the mitochondrial trifunctional protein MTP and the respiratory chain supercomplexes by mutated EHHADH. This leads to decreased oxidative phosphorylation, an accumulation of acylcarnitines, and decreased mitochondrial energy production in proximal tubular cells, all of which contribute to decreased reabsorption of electrolytes and low-molecular-weight nutrients, a characteristic of renal Fanconi syndrome (Figure 4).

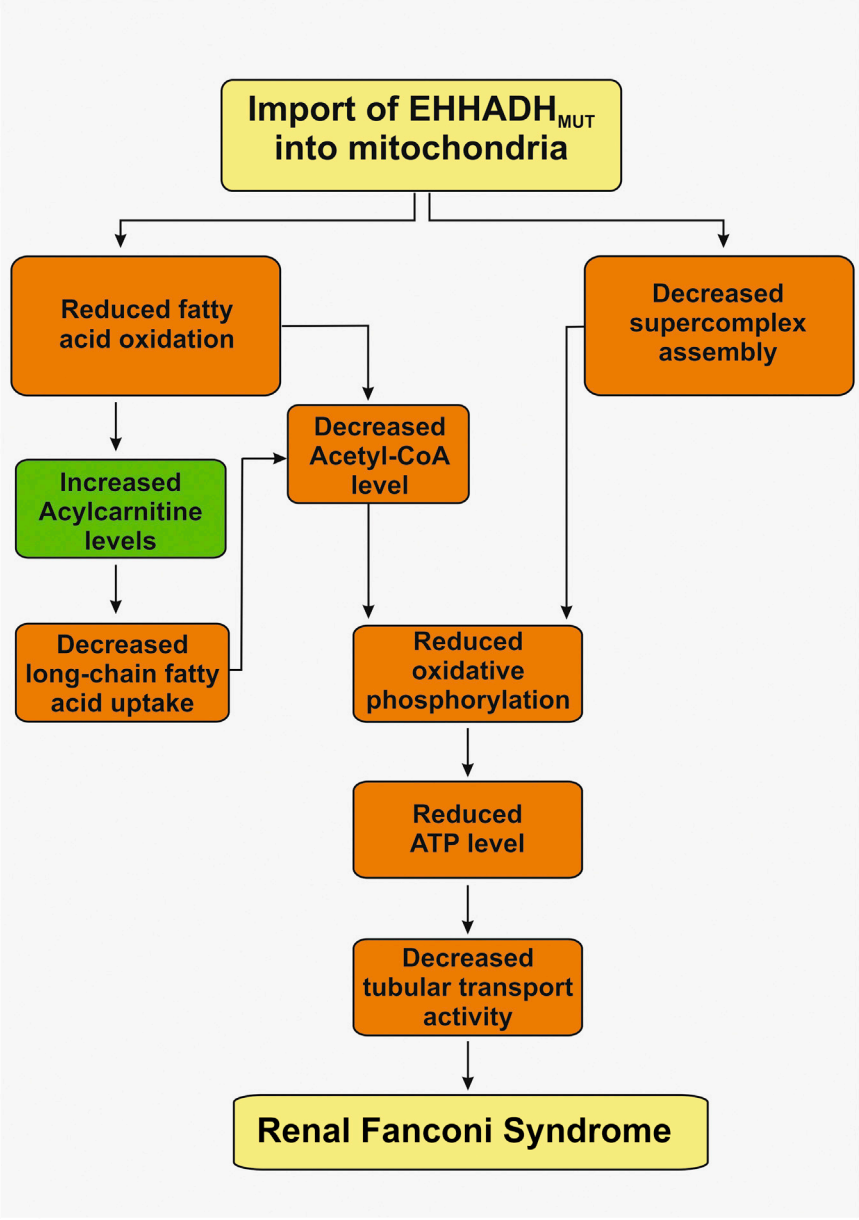

Figure 4. Effect of Mistargeted EHHADH$_{MUT}$ on Mitochondrial Function

The import of EHHADH$_{MUT}$ into mitochondria and incorporation into the MTP complex leads to a reduction of MTP activity and a decreased supercomplex assembly. Both result in reduced oxidative phosphorylation, which decreases the intracellular ATP level. This, in turn, decreases proximal tubular transport and, consequently, causes Fanconi syndrome (green/orange, up/downregulation).

EXPERIMENTAL PROCEDURES

LLC-PK1 cells stably transfected with either *EHHADH$_{WT}$* or *EHHADH$_{MUT}$* cDNA using the Tet-On inducible gene expression system (Klootwijk et al., 2014) were used for all studies, with 7 days of stimulation. Cells were harvested by scraping in ice-cold methanol. In case of isolation of mitochondria by differential centrifugation and co-immunoprecipitation using protein A/G magnetic beads, cells were harvested by trypsination. All metabolite analyses were accomplished using GC- or LC-MS. ATP and apoptosis measurements were conducted using commercially available kits. Mass spectrometrical protein analyses for protein interactions and label-free, differential analysis were done using nano-LC- quadrupole time of flight-MS. For analysis of Na^+/K^+-ATPase activity, Rb^+ was used as a K^+ surrogate and measured by ICP-OES. For respirometry, confocal microscopy, and detailed method descriptions, see the Supplemental Experimental Procedures. Comparisons between groups were made using Student's t tests. $p \leq 0.05$ was considered statistically significant. In case of multiple testing, p values were adjusted by controlling the false discovery rate (Benjamini and Hochberg, 1995). In all figures, $^*p \leq 0.05$, $^{**}p \leq 0.01$, and $^{***}p \leq 0.001$.

SUPPLEMENTAL INFORMATION

Supplemental Information includes Supplemental Experimental Procedures, two figures, and three tables and can be found with this article online at http://dx.doi.org/10.1016/j.celrep.2016.04.037.

AUTHOR CONTRIBUTIONS

Conceptualization, J.R., M.R., and R.K.; Methodology, J.R., M.R., K.D., K.R.S., A.H., and A.D.; Investigation, N.A., J.M.B.S., C.B., H.C., N.N., and

E.K.; Writing, N.A. and J.R.; Review and Editing, J.R. and M.R.; Resources, P.J.O.; Supervision, P.J.O. and R.K.; Funding Acquisition, M.R., J.R., P.J.O., and R.K.

ACKNOWLEDGMENTS

This work was supported by Deutsche Forschungsgemeinschaft Grant SFB699 TP-A11, BayGene, the European Commission Seventh Framework Programme (2012-305608 European Consortium for High-Throughput Research in Rare Kidney Diseases), and the Lowe Syndrome Trust. The authors thank Sciex for instrumental support, Dr. Gruber (University Clinic Regensburg) for providing equipment for CO_2 analysis, and Dr. Krischke (University Würzburg) for helpful advice and discussions.

Received: November 3, 2014
Revised: February 28, 2016
Accepted: April 5, 2016
Published: May 5, 2016

REFERENCES

Andreoli, S.P., and Mallett, C.P. (1997). Disassociation of oxidant-induced ATP depletion and DNA damage from early cytotoxicity in LLC-PK1 cells. Am. J. Physiol. *272*, F729–F735.

Balaban, R.S., Mandel, L.J., Soltoff, S.P., and Storey, J.M. (1980). Coupling of active ion transport and aerobic respiratory rate in isolated renal tubules. Proc. Natl. Acad. Sci. USA *77*, 447–451.

Beck, J.S., Breton, S., Mairbäurl, H., Laprade, R., and Giebisch, G. (1991). Relationship between sodium transport and intracellular ATP in isolated perfused rabbit proximal convoluted tubule. Am. J. Physiol. *261*, F634–F639.

Benjamini, Y., and Hochberg, Y. (1995). Controlling the false discovery rate: a practical and powerful approach to multiple testing. J. R. Statist. Soc. B *57*, 289–300.

Curthoys, N.P., and Moe, O.W. (2014). Proximal tubule function and response to acidosis. Clin. J. Am. Soc. Nephrol. *9*, 1627–1638.

Eaton, S. (2002). Control of mitochondrial beta-oxidation flux. Prog. Lipid Res. *41*, 197–239.

Epstein, F.H. (1997). Oxygen and renal metabolism. Kidney Int. *51*, 381–385.

Gillingham, M.B., Scott, B., Elliott, D., and Harding, C.O. (2006). Metabolic control during exercise with and without medium-chain triglycerides (MCT) in children with long-chain 3-hydroxy acyl-CoA dehydrogenase (LCHAD) or trifunctional protein (TFP) deficiency. Mol. Genet. Metab. *89*, 58–63.

Gorvin, C.M., Wilmer, M.J., Piret, S.E., Harding, B., van den Heuvel, L.P., Wrong, O., Jat, P.S., Lippiat, J.D., Levtchenko, E.N., and Thakker, R.V. (2013). Receptor-mediated endocytosis and endosomal acidification is impaired in proximal tubule epithelial cells of Dent disease patients. Proc. Natl. Acad. Sci. USA *110*, 7014–7019.

Hirschey, M.D., Shimazu, T., Goetzman, E., Jing, E., Schwer, B., Lombard, D.B., Grueter, C.A., Harris, C., Biddinger, S., Ilkayeva, O.R., et al. (2010). SIRT3 regulates mitochondrial fatty-acid oxidation by reversible enzyme deacetylation. Nature *464*, 121–125.

Ho, C.H., and Pande, S.V. (1974). On the specificity of the inhibition of adenine nucleotide translocase by long chain acyl-coenzyme A esters. Biochim. Biophys. Acta *369*, 86–94.

Hoefler, G., Forstner, M., McGuinness, M.C., Hulla, W., Hiden, M., Krisper, P., Kenner, L., Ried, T., Lengauer, C., Zechner, R., et al. (1994). cDNA cloning of the human peroxisomal enoyl-CoA hydratase: 3-hydroxyacyl-CoA dehydrogenase bifunctional enzyme and localization to chromosome 3q26.3-3q28: a free left Alu Arm is inserted in the 3′ noncoding region. Genomics *19*, 60–67.

Ivanova, E.A., De Leo, M.G., Van Den Heuvel, L., Pastore, A., Dijkman, H., De Matteis, M.A., and Levtchenko, E.N. (2015). Endo-lysosomal dysfunction in human proximal tubular epithelial cells deficient for lysosomal cystine transporter cystinosin. PLoS ONE *10*, e0120998.

Klootwijk, E.D., Reichold, M., Helip-Wooley, A., Tolaymat, A., Broeker, C., Robinette, S.L., Reinders, J., Peindl, D., Renner, K., Eberhart, K., et al. (2014). Mistargeting of peroxisomal EHHADH and inherited renal Fanconi's syndrome. N. Engl. J. Med. *370*, 129–138.

Migita, K., Zhao, Y., and Katsuragi, T. (2007). Mitochondria play an important role in adenosine-induced ATP release from Madin-Darby canine kidney cells. Biochem. Pharmacol. *73*, 1676–1682.

Novarino, G., Weinert, S., Rickheit, G., and Jentsch, T.J. (2010). Endosomal chloride-proton exchange rather than chloride conductance is crucial for renal endocytosis. Science *328*, 1398–1401.

Reddy, J.K., and Hashimoto, T. (2001). Peroxisomal beta-oxidation and peroxisome proliferator-activated receptor alpha: an adaptive metabolic system. Annu. Rev. Nutr. *21*, 193–230.

Rinaldo, P., Cowan, T.M., and Matern, D. (2008). Acylcarnitine profile analysis. Genet. Med. *10*, 151–156.

Rosca, M.G., Vazquez, E.J., Kerner, J., Parland, W., Chandler, M.P., Stanley, W., Sabbah, H.N., and Hoppel, C.L. (2008). Cardiac mitochondria in heart failure: decrease in respirasomes and oxidative phosphorylation. Cardiovasc. Res. *80*, 30–39.

Sander, J., Sander, S., Steuerwald, U., Janzen, N., Peter, M., Wanders, R.J., Marquardt, I., Korenke, G.C., and Das, A.M. (2005). Neonatal screening for defects of the mitochondrial trifunctional protein. Mol. Genet. Metab. *85*, 108–114.

Saudubray, J.M., Martin, D., de Lonlay, P., Touati, G., Poggi-Travert, F., Bonnet, D., Jouvet, P., Boutron, M., Slama, A., Vianey-Saban, C., et al. (1999). Recognition and management of fatty acid oxidation defects: a series of 107 patients. J. Inherit. Metab. Dis. *22*, 488–502.

Schägger, H. (2001). Respiratory chain supercomplexes. IUBMB Life *52*, 119–128.

Shrago, E., Woldegiorgis, G., Ruoho, A.E., and DiRusso, C.C. (1995). Fatty acyl CoA esters as regulators of cell metabolism. Prostaglandins Leukot. Essent. Fatty Acids *52*, 163–166.

Tonin, A.M., Amaral, A.U., Busanello, E.N., Grings, M., Castilho, R.F., and Wajner, M. (2013). Long-chain 3-hydroxy fatty acids accumulating in long-chain 3-hydroxyacyl-CoA dehydrogenase and mitochondrial trifunctional protein deficiencies uncouple oxidative phosphorylation in heart mitochondria. J. Bioenerg. Biomembr. *45*, 47–57.

Ventura, F.V., Ruiter, J.P., Ijlst, L., Almeida, I.T., and Wanders, R.J. (1995). Inhibition of oxidative phosphorylation by palmitoyl-CoA in digitonin permeabilized fibroblasts: implications for long-chain fatty acid beta-oxidation disorders. Biochim. Biophys. Acta *1272*, 14–20.

Ventura, F.V., Ruiter, J.P., Ijlst, L., de Almeida, I.T., and Wanders, R.J. (1996). Inhibitory effect of 3-hydroxyacyl-CoAs and other long-chain fatty acid beta-oxidation intermediates on mitochondrial oxidative phosphorylation. J. Inherit. Metab. Dis. *19*, 161–164.

Ventura, F.V., Ijlst, L., Ruiter, J., Ofman, R., Costa, C.G., Jakobs, C., Duran, M., Tavares de Almeida, I., Bieber, L.L., and Wanders, R.J. (1998). Carnitine palmitoyltransferase II specificity towards beta-oxidation intermediates–evidence for a reverse carnitine cycle in mitochondria. Eur. J. Biochem. *253*, 614–618.

Violante, S., Ijlst, L., Te Brinke, H., Tavares de Almeida, I., Wanders, R.J., Ventura, F.V., and Houten, S.M. (2013). Carnitine palmitoyltransferase 2 and carnitine/acylcarnitine translocase are involved in the mitochondrial synthesis and export of acylcarnitines. FASEB J. *27*, 2039–2044.

Wang, Y., Mohsen, A.W., Mihalik, S.J., Goetzman, E.S., and Vockley, J. (2010). Evidence for physical association of mitochondrial fatty acid oxidation and oxidative phosphorylation complexes. J. Biol. Chem. *285*, 29834–29841.